Probing BSA Binding to Citrate-Coated Gold Nanoparticles and Surfaces

Scott H. Brewer,[†] Wilhelm R. Glomm,[‡] Marcus C. Johnson,[†] Magne K. Knag,[‡] and Stefan Franzen*,[†]

Department of Chemistry, North Carolina State University, Raleigh, North Carolina 27695, and Ugelstad Laboratory, Department of Chemical Engineering, Norwegian University of Science and Technology, N-7491 Trondheim, Norway

Received March 4, 2005. In Final Form: June 25, 2005

The interaction of bovine serum albumin (BSA) with gold colloids and surfaces was studied using ζ-potential and quartz crystal microbalance (QCM) measurements, respectively, to determine the surface charge and coverage. The combination of these two measurements suggests that BSA binding to gold nanoparticles and gold surfaces occurs by an electrostatic mechanism when citrate is present. The binding of BSA to bare gold is nearly two times greater than the binding of BSA to a citrate-coated gold surface, suggesting that protein spreading (denaturation) on the surface may occur followed by secondary protein binding. On the other hand, binding to citrate-coated gold surfaces can be fit to a Langmuir isotherm model to obtain a maximum surface coverage of $(3.7 \pm 0.2) \times 10^{12}$ molecules/cm^2 and a binding constant of $1.0 \pm 0.3\ \mu M^{-1}$. The ζ-potential measurements show that the stabilization of colloids by BSA has a significant contribution from a steric mechanism because the colloids are stable, even at their isoelectric point (pI ≈ 4.6). To be consistent with the observed phenomena, the electrostatic interactions between BSA and citrate must consist of salt-bridges, for example, of the carboxylate−ammonium type, between the citrate and the lysine on the protein surface. The data support the role of strong electrostatic binding but do not exclude contributions from steric or hydrophobic interactions with the surface adlayer.

Introduction

Gold nanoparticles have been widely used as cell-targeting vectors[1−9] and in bioassays, such as in the detection of DNA hybridization,[10,11] to take advantage of their unique optical and electronic properties. Citrate is a common electrostatic stabilizing agent for gold nanoparticles because the particles are typically synthesized through a citric acid reduction reaction.[12−14] Electrostatic stabilization arises from a mutual repulsion between neighboring gold nanoparticles that occurs as a result of the negative surface charge of the citrate layer. Citrate has also been used as a stabilizing agent for alumina particles.[15] Gold nanoparticles have been modified with bovine serum albumin (BSA) for cell-targeting applications. BSA appears to bind spontaneously to the surface of citrate-coated gold nanoparticles; however, the mechanism of its binding has not yet been determined. Studies of the binding of BSA to gold surfaces reveal that nonspecific binding to self-assembled monolayers is favored in the following order: hydrophobic > COO^- > NH_3^+ > OH > ethylene glycol.[16−18] The adhesion force of BSA binding to silica surfaces has been measured.[19] In

* To whom correspondence should be addressed. Phone: (919) 515-8915; fax: (919) 515-8909; e-mail: Stefan_Franzen@ncsu.edu.

† North Carolina State University.

‡ Norwegian University of Science and Technology.

(1) Tkachenko, A. G.; Xie, H.; Coleman, D.; Glomm, W.; Ryan, J.; Anderson, M. F.; Franzen, S.; Feldheim, D. L. Multifunctional Gold Nanoparticle−Peptide Complexes for Nuclear Targeting. *J. Am. Chem. Soc.* **2003**, *125* (16), 4700−4701.

(2) Tkachenko, A. G.; Xie, H.; Liu, Y. L.; Coleman, D.; Ryan, J.; Glomm, W. R.; Shipton, M. K.; Franzen, S.; Feldheim, D. L. Cellular Trajectories of Peptide-Modified Gold Particle Complexes: Comparison of Nuclear Localization Signals and Peptide Transduction Domains. *Bioconjugate Chem.* **2004**, *15* (3), 482−490.

(3) Tkachenko, A. G.; Xie, H.; Ryan, J.; Glomm, W. R.; Franzen, S.; Feldheim, D. L. Assembly and Characterization of Biomolecule−Gold Nanoparticle Conjugates and Their Use in Intracellular Imaging. In *Bionanotechnology Protocols*; Rosenthal, S., Wright, D., Eds.; Humana Press: New York, in press.

(4) Xie, H.; Tkachenko, A. G.; Glomm, W. R.; Ryan, J. A.; Brennaman, M. K.; Papanikolas, J. M.; Franzen, S.; Feldheim, D. L. Critical Flocculation Concentrations, Binding Isotherms, and Ligand Exchange Properties of Peptide-Modified Gold Nanoparticles Studied by UV−Visible, Fluorescence, and Time-Correlated Single Photon Counting Spectroscopies. *Anal. Chem.* **2003**, *75* (21), 5797−5805.

(5) Feldherr, C. M.; Akin, D. The Permeability of the Nuclear-Envelope in Dividing and Nondividing Cell-Cultures. *J. Cell Biol.* **1990**, *111* (1), 1−8.

(6) Feldherr, C. M.; Lanford, R. E.; Akin, D. Signal-Mediated Nuclear Transport in Simian-Virus 40-Transformed Cells Is Regulated by Large Tumor-Antigen. *Proc. Natl. Acad. Sci. U.S.A.* **1992**, *89* (22), 11002−11005.

(7) Feldherr, C. M.; Akin, D. Variations in Signal-Mediated Nuclear Transport During the Cell-Cycle in Balb/C 3t3 Cells. *Exp. Cell Res.* **1994**, *215* (1), 206−210.

(8) Feldherr, C.; Akin, D. Nuclear Transport in Amoebae. *Mol. Biol. Cell* **1998**, *9*, 188A-188A.

(9) Feldherr, C. M.; Akin, D. Signal-Mediated Nuclear Transport in the Amoeba. *J. Cell Sci.* **1999**, *112* (12), 2043−2048.

(10) Demers, L. M.; Mirkin, C. A.; Mucic, R. C.; Reynolds, R. A.; Letsinger, R. L.; Elghanian, R.; Viswanadham, G. A Fluorescence-Based Method for Determining the Surface Coverage and Hybridization Efficiency of Thiol-Capped Oligonucleotides Bound to Gold Thin Films and Nanoparticles. *Anal. Chem.* **2000**, *72* (22), 5535−5541.

(11) Taton, T. A.; Mirkin, C. A.; Letsinger, R. L., Scanometric DNA Array Detection with Nanoparticle Probes. *Science* **2000**, *289* (5485), 1757−1760.

(12) Turkevich, J.; Stevenson, P. C.; Hillier, J. A Study of the Nucleation and Growth Processes in the Synthesis of Colloidal Gold. *Discuss. Faraday Soc.* **1951**, *11*, 55−59.

(13) Turkevich, J.; Stevenson, P. C.; Hillier, J. The Formation of Colloidal Gold. *J. Phys. Chem.* **1953**, *57* (7), 670−673.

(14) Turkevich, J.; Garton, G.; Stevenson, P. C. The Color of Colloidal Gold. *J. Colloid Sci.* **1954**, *9* (6), S26−S35.

(15) Hidber, P. C.; Graule, T. J.; Gauckler, L. J. Citric Acid − A Dispersant for Aqueous Alumina Suspensions. *J. Am. Ceram. Soc.* **1996**, *79* (7), 1857−1867.

(16) Nakata, S.; Kido, N.; Hayashi, M.; Hara, M.; Sasabe, H.; Sugawara, T.; Matsuda, T. Chemisorption of Proteins and Their Thiol Derivatives onto Gold Surfaces: Characterization Based on Electrochemical Nonlinearity. *Biophys. Chem.* **1996**, *62* (1−3), 63−72.

(17) Silin, V.; Weetall, H.; Vanderah, D. J. SPR Studies of the Nonspecific Adsorption Kinetics of Human IgG and BSA on Gold Surfaces Modified by Self-Assembled Monolayers (SAMs). *J. Colloid Interface Sci.* **1997**, *185* (1), 94−103.

10.1021/la050588t CCC: $30.25
Published on Web 08/20/2005

these studies, it is clear that BSA has a preference for binding to negatively charged surfaces. However, the preferential binding of BSA to negatively charged surfaces is somewhat puzzling because the isoelectric point of BSA is 4.6, and therefore BSA is negatively charged at pH 7.0, which is the pH at which many experiments are carried out. Regardless of the overall charge, BSA has 60 surface lysine groups that can have electrostatic interactions with negatively charged moieties. BSA can be conjugated to other proteins and peptides utilizing the large number of surface lysine residues of BSA as a scaffold for chemical attachment.[1−4] The use of gold nanoparticles allows for tracking the bioconjugate (nanoparticle plus coating) in different cellular compartments, the cytosol, or the nucleus by the use of optical microscopy and transmission electron microscopy (TEM).[1−9] These uses for BSA increase the interest in understanding the specific mechanism whereby BSA attaches to surfaces.

Quantification of protein adsorption on colloids or nanoparticles is a challenging problem. Measurements of BSA on magnetic[20] and aluminum oxide[21] nanoparticles have been reported. Two possible mechanisms of BSA binding to nanoparticles have been suggested: either "end-on" or "side-on" binding, in which end-on binding results in a higher surface coverage of BSA on the surface. Proteins can be attached to the surface by chemical cross-linking reagents, or they can spontaneously assemble because of the electrostatic forces. In the layer-by-layer approach, the binding of a protein to the surface of a colloid is achieved by electrostatic interactions.[22] However, self-assembly can also occur by protein denaturation onto the surface.

During the formation of an adsorbed layer on a surface, each adsorbing molecule must pass through the following steps: (1) transport toward the surface, (2) attachment to the surface, and (3) spreading on the surface.[23] These steps are consistent with the two possible hypotheses for the interaction between BSA and a citrate-coated gold surface or a nanoparticle. The first is an electrostatic binding hypothesis and the second is a displacement hypothesis. The electrostatic binding hypothesis states that the attraction between the positive surface residues (at basic pH values) of BSA and the negative charge from the citrate are responsible for the strong binding of BSA to citrate-coated gold nanoparticles. In this hypothesis, the protein attaches itself to the passivating layer on the gold surface, with little direct interaction between BSA and the gold surface. The displacement hypothesis requires citrate to be displaced by BSA upon adsorption, with the amino acids (functional groups) lysine (amine), histidine (imidazole), and cysteine (thiol) among others that interact directly with the gold surface. Spreading or structural changes in the adsorbing protein on the surface can lower the free energy of the system. Changes in protein structure are most often the result of denaturation that occurs during the displacement of the citrate stabilizer. Consequently, the displacement hypothesis can be divided into two possible outcomes: (1) displacement by the protein in its native structure and (2) denaturation of the protein on the surface. If denaturation occurs during displacement, then the protein unfolds near the surface and exposes hydrophobic residues and presents specific functional groups that interact with the gold surface. Dispersive and van der Waals forces must play some role in all of the above mechanisms as well.

The interaction of the protein with a colloid surface can involve these two possibilities, but the steric interactions of a protein with a surface layer, such as citrate, can provide greater colloidal stability to a colloid than pure electrostatic interaction. For example, electrostatic stabilization alone will fail to stabilize the colloid at the isoelectric point. However, protein-coated colloidal suspensions can be stabilized by the interaction of protein side chains or domains, which results in a reduction in entropy and a loss of solvation enthalpy, both of which result in an intercolloid repulsion.

Small changes in the surface structure can profoundly affect the stability of the colloidal suspension. Thus, the quantitative study of protein interaction with surface adlayers is difficult at best. We propose using two techniques to study colloids and gold surfaces to understand the surface binding mechanism of BSA as a prototypical and widely used protein. To better understand citrate- and BSA-coated gold nanoparticles and surfaces, we used a quartz crystal microbalance (QCM) to measure citrate and BSA binding isotherms to gold surfaces. Because our goal is to understand how protein binding affects colloidal stability, we combined the protein isotherm measurements with ζ-potential measurements, which include the pH dependence of the surface charge of citrate- and BSA-coated 10-nm gold nanoparticles. This combination of techniques provides a remarkably robust analysis of the interaction of the protein BSA with the stabilizing citrate surface layer without requiring the use of modified proteins, such as luminescent or radioactive labeled proteins, in the detection strategy.

A quartz crystal microbalance with dissipation (QCM-D) monitors both the frequency change upon binding to a gold surface and the dissipation change (the frictional and viscoelastic energy losses in the system) upon binding. Kasemo and co-workers pioneered the use of QCM-D for studying biological surface science-related processes in liquids,[24] including protein adsorption on pure[25,26] and phospholipid-coated[27] surfaces, the adsorption of transmembrane proteins containing supported phospholipid bilayers on silica,[28] intact vesicle adsorption and supported biomembrane formation from vesicles in solution,[29] and cell adhesion on supported lipid bilayers.[30] Comparative

(18) Moulin, A. M.; O'Shea, S. J.; Badley, R. A.; Doyle, P.; Welland, M. E. Measuring Surface-Induced Conformational Changes in Proteins. *Langmuir* **1999**, *15* (26), 8776−8779.

(19) Valle-Delgado, J. J.; Molina-Bolivar, J. A.; Galisteo-Gonzalez, F.; Galvez-Ruiz, M. J.; Feiler, A.; Rutland, M. W. Interaction Forces between BSA Layers Adsorbed on Silica Surfaces Measured with an Atomic Force Microscope. *J. Phys. Chem. B* **2004**, *108* (17), 5365−5371.

(20) Peng, Z. G.; Hidajat, K.; Uddin, M. S. Adsorption of Bovine Serum Albumin on Nanosized Magnetic Particles. *J. Colloid Interface Sci.* **2004**, *271* (2), 277−283.

(21) Rezwan, K.; Meier, L. P.; Rezwan, M.; Voros, J.; Textor, M.; Gauckler, L. J. Bovine Serum Albumin Adsorption onto Colloidal Al_2O_3 Particles: A New Model Based on Zeta Potential and UV−Vis Measurements. *Langmuir* **2004**, *20* (23), 10055−10061.

(22) Stein, E. W.; McShane, M. J. Multilayer Lactate Oxidase Shells on Colloidal Carriers as Engines for Nanosensors. *IEEE Trans. Nanobioscience* **2003**, *2* (3), 133−137.

(23) Malmsten, M. *Biopolymers at Interfaces*, 2nd ed.; Marcel Dekker: New York, 2003; Vol. 110.

(24) Kasemo, B. Biological Surface Science. *Surf. Sci.* **2002**, *500* (1−3), 656−677.

(25) Hook, F.; Kasemo, B.; Nylander, T.; Fant, C.; Sott, K.; Elwing, H. Variations in Coupled Water, Viscoelastic Properties, and Film Thickness of a Mefp-1 Protein Film During Adsorption and Cross-Linking: A Quartz Crystal Microbalance with Dissipation Monitoring, Ellipsometry, and Surface Plasmon Resonance Study. *Anal. Chem.* **2001**, *73* (24), 5796−5804.

(26) Hook, F.; Voros, J.; Rodahl, M.; Kurrat, R.; Boni, P.; Ramsden, J. J.; Textor, M.; Spencer, N. D.; Tengvall, P.; Gold, J.; Kasemo, B. A Comparative Study of Protein Adsorption on Titanium Oxide Surfaces Using In Situ Ellipsometry, Optical Waveguide Lightmode Spectroscopy, and Quartz Crystal Microbalance/Dissipation. *Colloids Surf., B* **2002**, *24* (2), 155−170.

(27) Glasmastar, K.; Larsson, C.; Hook, F.; Kasemo, B. Protein Adsorption on Supported Phospholipid Bilayers. *J. Colloid Interface Sci.* **2002**, *246* (1), 40−47.

studies of protein adsorption using QCM-D and optical techniques, such as ellipsometry, surface plasmon resonance (SPR) and optical waveguide lightmode spectroscopy (OWL), have shown that the values measured by QCM-D are generally higher in terms of mass than those measured by the corresponding optical techniques because the frequency change in liquid QCM-D is sensitive to both protein adsorption and water molecules that bind or hydrodynamically couple to the protein adlayer.[25,26] However, QCM-D is complementary to optical techniques because it provides insight into the mechanical and structural properties of the adlayer. The study of viscoelasticity through the analysis of the energy dissipation in the adlayer can be related to the magnitude of the frequency shift (due to the adsorbed mass).

Materials and Methods

Sodium citrate (referred to as citrate) and BSA were received from Mallinckrodt Chemical and Sigma-Aldrich, respectively. The 10-nm gold nanoparticles were received from BBInternational.

The QCM-D [Q-Sense (Gothenburg, Sweden)] studies used quartz crystals coated with gold that had a fundamental frequency of 5 MHz. The fundamental, along with the third, fifth, and seventh harmonic of the fundamental frequency, was monitored as a function of time to determine the change in frequency of the crystal upon the addition of the analyte. The average of the frequency change of the third, fifth, and seventh harmonics were averaged to estimate the error in the measurements. The dissipation change was also recorded as a function of time upon analyte addition. The experiments were performed at room temperature. We distinguished two experimental protocols. In the direct deposition measurement, a BSA solution was deposited onto a freshly prepared citrate-coated gold slide for each measurement. In the sequential deposition measurement, successive aliquots of BSA were added sequentially to a single gold-coated crystal, ranging from low to high concentration, and a citrate buffer wash was performed after each measurement. Sequential deposition is convenient because highly reproducible measurements can be obtained more readily once a good crystal is found and stable conditions have been achieved.

The ζ-potential (ZetaSizer 3000, Malvern Instruments) measurements of the 10-nm gold nanoparticles consisted of five repeats at each pH value to estimate the error in the measurements. The pH was varied from basic values to more acidic pH values in increments of approximately one pH unit. The measurements were recorded at room temperature. Because the ζ-potential measurements were performed in an aqueous solution, the Smoluchowski approximation was used to calculate the ζ-potentials from the measured electrophoretic mobilities.[31]

Results and Discussion

Figure 1A shows representative QCM-D results in the change of the 35-MHz seventh overtone of the fundamental frequency (5 MHz) and the dissipation change upon the sequential addition of citrate (10 mM in water, pH 8.55) and BSA (maximum concentration of 100 μM in 10 mM citrate in water) to a gold-coated quartz crystal. These results (normalized by dividing by a factor of 7, which corresponds to the number of the harmonic) show a decrease in the frequency of ~3.4 and 23.7 Hz and a change in the dissipation of 0.5 and 2.0 for the addition of citrate and BSA, respectively. This dissipation change is indicative of the formation of a nonrigid layer on the gold surface. The formation of a viscoelastic layer results in a change in the dissipated energy because it dampens the oscillation. These changes in the frequency and dissipation are due to the sequential binding of citrate and BSA to the gold surface. Figure 1B shows the BSA concentration dependence (1−100 μM) of the frequency change in response to the binding of BSA to a citrate-coated gold surface. The QCM-D measurements for each concentration of BSA were performed on separate gold-coated quartz crystals to determine the resulting surface coverage of BSA that corresponds to each solution concentration. The change in frequency was converted to an approximate surface coverage of BSA using the Sauerbrey equation:[32]

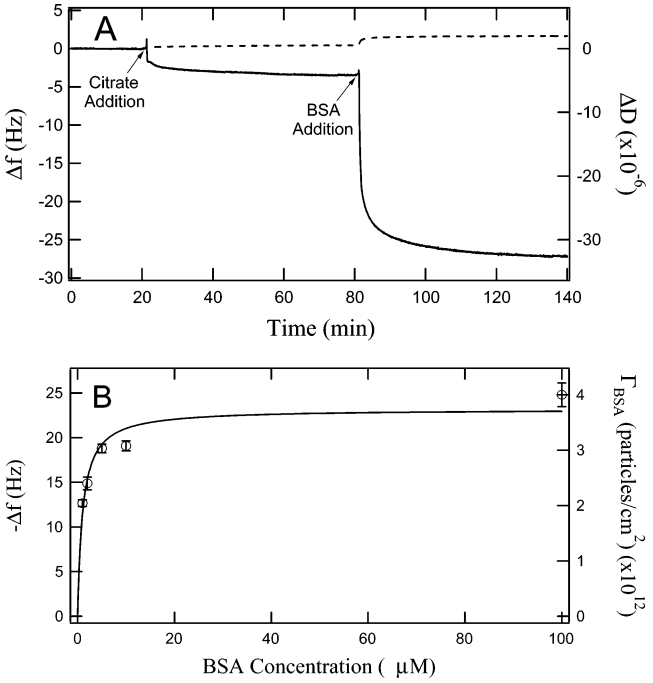

Figure 1. (A) Representative QCM-D-measured change in the frequency of the 35-MHz seventh harmonic of the fundamental frequency and dissipation change upon the binding of citrate (10 mM in water) and the subsequent binding of BSA (100 μM in 10 mM citrate in water) to a gold-coated quartz crystal as a function of time at 25.7 ± 0.1 °C. The raw data were divided by 7 to normalize for the use of the seventh harmonic in the QCM-D instrument. (B) The change in frequency (hollow circles) and the corresponding change in surface coverage for the direct deposition of BSA as a function of concentration onto a citrate-modified gold surface, fit (solid curve) to a Langmuir adsorption isotherm (eq 2). The data points are the result of the average frequency change of the third, fifth, and seventh harmonics of the resonance frequency with the corresponding standard deviations.

$$\Delta m = -\frac{C\Delta f}{n} \quad (1)$$

in which Δm is the change in mass, n is the number of the harmonic of the fundamental resonance frequency used in the experiment, Δf is the change in frequency, and C has a value of 17.8 ng/cm^2/Hz^1 for the crystals used in

(28) Graneli, A.; Rydstrom, J.; Kasemo, B.; Hook, F. Formation of Supported Lipid Bilayer Membranes on SiO_2 from Proteoliposomes Containing Transmembrane Proteins. *Langmuir* **2003**, *19* (3), 842−850.

(29) Reimhult, E.; Hook, F.; Kasemo, B. Intact Vesicle Adsorption and Supported Biomembrane Formation from Vesicles in Solution: Influence of Surface Chemistry, Vesicle Size, Temperature, and Osmotic Pressure. *Langmuir* **2003**, *19* (5), 1681−1691.

(30) Andersson, A. S.; Glasmastar, K.; Sutherland, D.; Lidberg, U.; Kasemo, B. Cell Adhesion on Supported Lipid Bilayers. *J. Biomed. Mater. Res., Part A* **2003**, *64* (4), 622−629.

(31) Magdassi, S.; Bassa, A.; Vinetsky, Y.; Kamyshny, A. Silver Nanoparticles as Pigments for Water-Based Ink-Jet Inks. *Chem. Mater.* **2003**, *15* (11), 2208−2217.

(32) Sauerbrey, G. Verwendung Von Schwingquarzen Zur Wagung Dunner Schichten Und Zur Mikrowagung. *Z. Phys.* **1959**, *155* (2), 206−222.

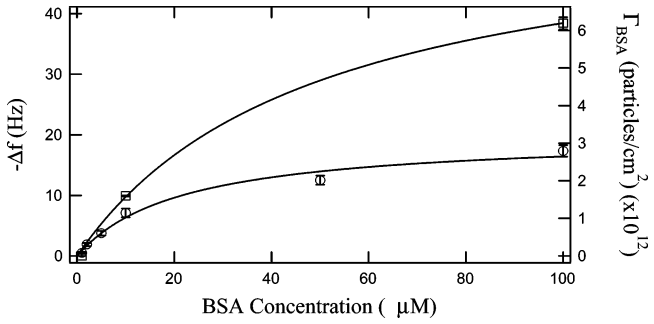

Figure 2. The change in the frequency of a gold-coated quartz crystal as a function of BSA concentration, coated with (hollow circles) or without (hollow squares) citrate, fit to a Langmuir adsorption isotherm (solid curve) (eq 2) measured at 25.7 ± 0.1 °C. These measurements were carried out as sequential depositions with a wash between each deposition step. The data points are the average values of the frequency change in the third, fifth, and seventh harmonics of the resonance frequency with the corresponding standard deviations.

these experiments. The Sauerbrey equation was used because the dissipated energy was less than 10^{-6} per 5 Hz of frequency change, as reported in previous studies.[25,26] The mass calculated from the frequency change is only an approximation because the frequency change is due to bound protein and any trapped or associated water molecules as well. The resulting surface coverage values as a function of BSA concentration in Figure 1B were subsequently fitted to the Langmuir adsorption isotherm given in eq 2:[33]

$$\Gamma_{BSA} = \frac{\Gamma_{max} K_L [S]_{free}}{1 + K_L [S]_{free}} \quad (2)$$

in which Γ_{BSA} is the surface coverage of BSA, Γ_{max} is the maximum coverage of BSA and K_L is a binding constant that corresponds to the inverse of the BSA solution concentration that is required to obtain one-half of Γ_{max}. We apply the Langmuir isotherm model in this study with the understanding that contributions due to spreading (protein denaturation) imply that the system is no longer in equilibrium, as required by the Langmuir binding model. Spreading tends to reduce the apparent binding constant because it results in a protein that binds irreversibly to the surface and blocks subsequent protein adsorption. With this caveat, we use the model for comparison of the direct (Figure 1B) and sequential (Figure 2) binding studies. The fit of the Langmuir model to the direct deposition binding data in Figure 1B gave the values of $(3.7 \pm 0.2) \times 10^{12}$ molecules/cm^2 for Γ_{max} and 1.0 ± 0.3 μM^{-1} for K_L. It is believed that the Langmuir model is most valid for the direct deposition measurements because there are no prior wash steps that can lead to irreversible protein interactions with the surface.

The sequential deposition measurements shown in Figure 2 are much easier to perform than those shown in Figure 1; however, they are less quantitative because the lack of the complete removal of the protein during the wash step changes the state of the system prior to each subsequent protein concentration. We used sequential deposition studies to perform control QCM-D binding studies of BSA to noncitrate-modified gold surfaces. Figure 2 shows the change in the frequency and surface coverage of BSA for citrate- (hollow circles) and noncitrate- (hollow squares) coated gold surfaces as a function of BSA concentration fitted to a Langmuir adsorption isotherm for comparison with Figure 1. These fits yielded values of $(3.2 \pm 0.3) \times 10^{12}$ and $(9.2 \pm 0.8) \times 10^{12}$ molecules/cm^2 for Γ_{max}, whereas K_L was found to be 0.05 ± 0.01 μM^{-1} and 0.02 ± 0.005 μM^{-1} for the citrate- and noncitrate-coated gold surface, respectively. We stress that the significance of these values is not necessarily in accordance with the Langmuir model, and therefore these fits are for qualitative comparison purposes only. Figure 2 shows that the presence of citrate on the gold surface limits the amount of adsorption of BSA onto the gold surface. Therefore, BSA does not significantly displace the citrate upon binding to the surface.

The difference between the data in Figure 1B (direct deposition of BSA) and the solid squares in Figure 2 (sequential deposition of BSA) can be understood best by comparing the fits to the Langmuir binding model using the equilibrium constant K_L as a parameter to estimate the strength of the interaction of the protein with the surface. On citrate surfaces, the maximum surface coverage of BSA is 16% larger for the direct deposition method, and the binding constant is approximately 21 times larger for the direct deposition method relative to the sequential deposition method. This difference is consistent with an electrostatic binding mechanism of BSA to the citrate-coated gold surface. In the direct deposition method, each concentration of BSA is exposed to a citrate-coated gold surface, with the maximum negative charge of the surface coming from the citrate, to interact with the positive charges of the surface lysine groups of BSA. This interaction or attraction is diminished in the sequential deposition method because the negative charge of the citrate-coated surface is partially shielded by previously bound BSA molecules. This shielding occurs for all of the concentrations of BSA after the initial exposure of the surface to BSA. The addition of BSA to the surface will minimize the surface charge generated from the surface-bound citrate molecules and therefore minimize the attraction of BSA (through the surface lysine groups) to the surface. This difference will affect the driving force for the electrostatic binding of BSA to the citrate-coated gold surface, as seen experimentally with a lower binding constant for the sequential deposition method compared to that of the direct deposition method. This model is in agreement with previous work that showed that the binding of BSA to a gold surface is sensitive to the functional group terminating the thiol molecule that is used to form a self-assembled monolayer on the gold surface before exposure to BSA.[17] To account for the maximum surface coverage difference between the deposition methods, the spreading of the BSA molecules on the surfaces needs to be considered. The spreading of the BSA molecules on the surface in the sequential method likely minimizes the available surface area for the additional binding of BSA molecules, unlike the direct deposition method in which only citrate is bound to the surface initially. Consequently, the time scale of the binding and spreading of BSA will compete to influence the surface coverage of BSA on the surface. Further evidence for an electrostatic binding mechanism is found in the difference between the binding of BSA to a citrate-coated or bare gold surface. The maximum surface coverage of BSA on bare gold is roughly twice that found using either the sequential or direct deposition of BSA on citrate. The larger surface coverage on gold suggests that another mechanism (denaturation) is occurring as BSA binds to a bare gold surface. Denaturation can lead to multilayers of proteins interacting through hydrophobic

(33) Kirk, J. S.; Bohn, P. W. Surface Adsorption and Transfer of Organomercaptans to Colloidal Gold and Direct Identification by Matrix Assisted Laser Desorption/Ionization Mass Spectrometry. *J. Am. Chem. Soc.* **2004**, *126* (18), 5920−5926.

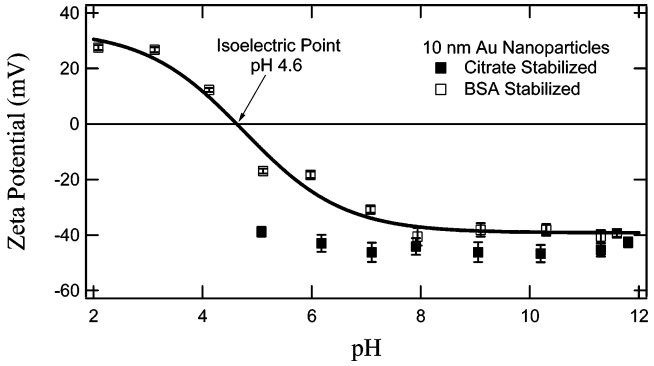

Figure 3. ζ-Potential of 10-nm gold nanoparticles recorded as a function of the stabilizing agent (citrate or BSA) and pH. The average ζ-potentials are plotted with error bars representing the standard deviations on the basis of five measurements.

groups, which explains the higher surface coverage. Although the surface coverage is higher for BSA on bare gold, the Langmuir binding constant is lower. The fact that the binding constant is significantly larger for a freshly prepared citrate-coated gold surface (see data in Figure 1) relative to that for a bare gold surface suggests that the binding of BSA to the citrate-coated gold surface proceeds predominately by an electrostatic mechanism.

Figure 3 shows the ζ-potential resulting from a pH titration of 10-nm gold nanoparticles (4.18×10^{12} particles/mL) that are stabilized by either citrate (solid squares) or BSA (hollow squares). The BSA-stabilized particles exhibited an isoelectric point (ζ-potential is zero) at pH 4.6, as determined by a sigmoid fit (solid curve) to the data of the BSA-modified nanoparticles. The commercially available citrate-stabilized gold nanoparticles were used as received, and the BSA-modified particles were obtained by mixing a BSA/gold nanoparticles solution in a ratio of 2000:1 for 16 h. In the control experiments, no measurable ζ-potential was obtained on BSA alone at the maximum concentration of 100 μM. Only in the presence of gold nanoparticles could a detectable ζ-potential be measured. The pH titration of the citrate-stabilized particles was stopped at pH 5 because of the onset of particle aggregation. BSA-coated particles were significantly more stable with respect to pH and thus allowed the isoelectric point (shown in Figure 3) of the BSA-coated gold nanoparticles to be measured. The ζ-potential data show that BSA imparts stability to the gold nanoparticles with respect to aggregation by both electrostatic (depending on the pH) forces and steric interactions. The stability imparted by steric interactions (bulky proteins on the surface preventing neighboring gold nanoparticles from getting in close enough proximity to interact and aggregate) is demonstrated by the fact that BSA-coated gold nanoparticles remain stable at the isoelectric point of the colloid. The nanoparticle suspension is least stable at the isoelectric point because electrostatic repulsion is at a minimum and attractive van der Waals interactions lead to particle flocculation. The citrate-stabilized gold nanoparticles show a slightly more negative ζ-potential than do the BSA-coated particles in the pH range in which they can be compared. The ζ-potential of the citrate particles ranged from −40 to −50 mV in the range of $5 < \text{pH} < 12$. Citrate-coated particles were unstable below pH 5. On the other hand, the ζ-potential of BSA-coated gold nanoparticles showed a strong pH dependence, starting at nearly −50 mV at pH 12 and decreasing to −20 mV by pH 5. Below pH 5 the ζ-potential continued to decrease, reaching the isoelectric point at pH 4.6 and further reaching a positive ζ-potential of +25 mV at pH 3. At the highest pH, it is not possible to prove that BSA is associated with the colloid surface. However, the QCM-D experiments show that, by pH 7, the BSA is associated with surface-bound citrate, although the effect on the ζ-potential is modest, which is consistent with a >15 mV less negative ζ-potential for the BSA-coated particles.

Conclusions

The combined QCM-D and ζ-potential experiments show that BSA binding to gold nanoparticles and gold surfaces occurs by an electrostatic mechanism. The ζ-potential measurements show that under conditions in which BSA is known to bind to the surface (on the basis of QCM-D), the ζ-potential is reduced compared to that of a similar particle with only a citrate coating. The fact that the protein binds even at the isoelectric point is consistent with an electrostatic mechanism. At pH 4.6, BSA has regions that act as a polycation because of the large number of protonated surface lysines. These groups can interact with citrate by salt-bridge interactions, even at the isoelectric point of the nanoparticle. The fact that BSA can readily dimerize and even form multimers may also suggest a greater degree of BSA association with the nanoparticle (i.e., formation of multilayers), although we have not studied this aspect further using these methods. The binding of BSA to a gold surface measured by QCM-D was found to decrease when the gold surface was first exposed to citrate relative to that measured on a clean surface. This result does not support the displacement hypothesis. If the citrate were significantly displaced, we would expect essentially the same result that was observed for bare gold. Moreover, we might also expect the high-pH form of the nanoparticles to show greater differences, which would indicate the displacement of surface citrate by BSA. Instead, both the QCM-D and ζ-potential measurements suggest that the *dominant* association of BSA with citrate-coated nanoparticles is electrostatic. The maximum surface coverage of $(3.7 \pm 0.2) \times 10^{12}$ molecules/cm^2 for BSA binding to citrate-coated gold surfaces (Figure 1B) implies that BSA is binding to the gold surface by an end-on mechanism. Assuming that the dimension of BSA are ($5.5 \times 5.5 \times 9$ nm),[21] then the binding of BSA in an end-on mechanism would be 3.3×10^{12} molecules/cm^2, whereas the binding by a side-on mechanism would be 2.0×10^{12} molecules/cm^2. The value obtained through the QCM experiments is slightly higher than the value for the surface coverage calculated by the end-on mechanism; however, this difference is likely due to the fact that the observed frequency change in the QCM studies is a function of both protein and bound water molecules and also to uncertainties arising from the Sauerbrey equation. This study offers the foundation for the future investigation of various modified metal nanoparticles with a variety of stabilizing agents and the subsequent binding of biomolecules, such as potential drug candidates, to these particles.

Acknowledgment. S.F. and S.B. gratefully acknowledge support by NSF Grant CHE-0436467, and M.J. acknowledges support by NSF Grant REU-0244181. We are grateful to Nancy Levinger at Colorado State University for her help in coordinating the international exchange project described in this work.

LA050588T